Characteristic Impedance and Parametric Variation effects on SWCNT bundle Interconnect at 22 nm Technology Node

Shailendra Mishra, R.P.Agarwal

***Abstract*— single walled carbon nanotubes (SWCNTs) holds extremely good electrical and mechanical properties in conjugation to their application in sub nanometer regime and a viable replacement to Cu interconnects. This indeed raises a need to realize their characteristic impedance and the analysis of their transient behavior under different mismatch conditions to optimize the performance of total circuitry. The paper intends to overview the safe amount of load mismatch tolerated by SWCNT bundles with configuration of varying lengths and diameters without any signal reliability issues.**

***Index Terms*— SWCNT bundle, Multi line interconnects, Characteristic Impedance, Transient analysis, Frequency analysis, Load mismatch, Multiple interconnect stacks.**

I. INTRODUCTION

In deep submicron regime more number of interconnections are used to connect millions of devices increasing wire resistance and giving rise to propagation delay. Earlier Al & Cu interconnects were viable enough, but the shrinking of device dimensions caused these conventional interconnects to suffer from problems like high electromigration resistance, surface roughness, grain boundary scattering, interconnect scaling, multiple interconnect stacks, leakage power, support to FinFET etc.

Carbon nanotubes (CNTs) offer an attractive option for VLSI interconnect applications as they have remarkable electrical, mechanical, thermal properties and large current-carrying capability due to their small dimensions [1]–[5]. This novel interconnect technology has the potential to replace copper in future. However, there occurs some significant technical barriers for using CNTs as building blocks in nanoelectronics [17]. Hence, a pragmatic analysis of the same becomes essential to evaluate their performance in the domain of on-chip interconnections.

This paper aims to derive an ideal model of SWCNT bundle as interconnect specific to 22nm technology. In doing so, a simplified representation of characteristic impedance along with its transient analysis is aimed with mismatch conditions to achieve performance optimization of total circuitry. The analysis gives an overview of safe amount of load mismatch tolerated by different lengths and diameters of interconnects without causing any signal reliability issues.

Manuscript received June 01, 2015

Shailendra Mishra, Department of electronics & Communication Engineering, Shobhit University, Meerut

R.P.Agarwal, Academic Advisor, Shobhit University, Meerut

II. PARAMETRIC CONSIDERATIONS FOR THE MODEL

SWCNT Transmission line model of an isolated CNT is modeled as a 1D quantum wire [6] as shown in fig. 1.

The interconnect parameters along with driver and load for SWCNT as interconnect are represented in fig. 2 where driver and load parameters are technology dependent [7].

The isolated SWCNTs has an intrinsic ballistic resistance of an approximate value of 6.453 kΩ which is independent of nanotube length [6] and expressed as:

$$R_Q = \frac{h}{4e^2} \quad (1)$$

This results in excessive delay for realistic interconnect applications which may be avoided considering bundled SWCNTs connected in parallel for all configurations such as local, intermediate, and global interconnects resulting in reduced intrinsic resistance . As a result, the TL theory has been extended to bundles of SWCNTs in the frequency domain.

Resistive losses also occur at the interface between the SWNT and the metal in the form of contact resistance R_C leading to current crowding at the edge of the metal contact resulting in a nonhomogeneous flow of current from the SWNT bundle to the metal [9, 15, 16]. Of all the different techniques considering the process variations in the contact resistance under various loading thermal annealing resulting in 40.7±0.7 Ω [8] is the preferred value of the contact resistance for the simulation setup presented in the paper.

Apart from R_C, CNTs with length $l > \lambda_{CNT}$ have scattering-induced ohmic resistance expressed as:

$$R_u = \frac{h}{4e^2}\frac{l}{\lambda_{mfp}} \text{ [6]} \quad (2)$$

hence, the total resistance exhibited by an isolated SWCNT is given as

$$R_{CNT} = R_C + R_Q + R_0 \quad (3)$$

The transmission line model of an isolated SWCNT also includes quantum capacitance C_Q Electrostatic capacitance C_E, kinetic inductance L_K and mutual inductance L_M given as:

$$C_Q = \frac{2e^2}{h v_f} \quad (4)$$

$$C_E = \frac{2\pi\varepsilon}{\ln(\frac{s}{d})} \quad (5)$$

$$L_K = \frac{h}{2e^2 v_f} \quad (6)$$

$$L_M = \frac{\mu_0}{2\pi}\ln(\frac{s}{d}) \quad (7)$$

The expressions for C_E and L_M are technology dependent. [6]. L_M is negligible at higher frequencies [6].

SWCNTs propose to be a good interconnect material as they are 1D conductors having a rich variety of low dimensional

charge transport phenomena, including ballistic conduction, localization and 1D variable range hopping [10]. The electron mean free path(λ_{mfp}), is one of the important length scales characterizing the different 1D transport regimes. It has been experimentally confirmed that λ_{mfp}, is generally much higher for MWCNTs than for SWCNTs indicating that the scattering of electrons is strongly suppressed in MWCNTs as predicted by Ando et al. [11] and McEuen et al. [12]. The value for λ_{mfp} obtained for the present paper is derived as:

$$\lambda_{mfp,i} = \frac{10^3 d_i}{\left(\frac{T}{T_0}\right)-2} \quad (8)$$

Here, $\lambda_{mfp,i}$ is the mean free path, di the diameter with respect to the ith shell, T_o =100K and T=300K (temperature to be considered for present simulation)

III. Physical Considerations for the Model

The MTL model for the present simulation considers the following conventions:

The SWCNT diameter is taken as d ≤ 2.5 nm to exclude any possibility of including MWCNT [13]

To form a VLSI interconnect, the CNTs must be bundled in order to reduce their large intrinsic resistance. One-third (Pm = 1/3) of the CNTs are metallic in a bundle. The remaining two-thirds are semiconducting and do not contribute to any current conduction.[6]

Considering densely packed SWCNT bundle the inter-CNT distance is considered to be:

$D = d+\delta$ (9) The concept can be convincingly visualized as depicted in fig. 3 where δ = 0.34nm and spacing = d0

All the physical dimensions such as width (w), height (h) separation (s) inter-CNT distance (D) are considered with respect to 22nm technology. [14]

Considering the above mentioned parametric values of isolated SWCNT the values of bundled SWCNT are derived using below mentioned formulae:

$$R_{Bundle} = \frac{R_{isolated}}{n_{CNT}} \quad (10)$$

$$L_{Bundle} = \frac{4}{P_m n_{CNT}} l \quad (11)$$

$$C_E^{Bundle} = 2C_E + \left(\frac{n_H-2}{2}\right) C_{EF} + \frac{3}{2}(n_H-2)C_E \quad (12)$$

$$C_Q^{Bundle} = 4C_Q(P_m n_{CNT})l \quad (13)$$

$$C_{Bundle} = \frac{C_E^{Bundle} + C_Q^{Bundle}}{C_E^{Bundle} \times C_Q^{Bundle}} \quad (14)$$

$$n_{CNT} = n_W n_H - \frac{n_H}{2} \text{ (even number of rows)} \quad (15)$$

$$n_{CNT} = n_W n_H - \frac{(n_H-1)}{2} \text{ (odd number of rows)} \quad (16)$$

$$n_H = \frac{(H-d)}{\sqrt{\frac{3}{2}}xy} + 1 \,,\; n_W = \frac{(w-d)}{y} \quad (17)$$

$$C_{EF} = \frac{2\pi\epsilon}{\ln\left(\frac{s+w}{d}\right)} \quad (18)$$

For the present paper the diameters considered for isolated SWCNT are 1nm, 2nm, 2.5 nm while length variations include 10µm, 15µm and 20µm considering local interconnect. Their corresponding values are incorporated in SWCNT bundle and are represented in figs. from fig. 4 to fig.6

IV. Characteristic Impedance of SWCNT Bundle Interconnects

Carbon nanotubes exhibit slow wave propagation and high characteristic impedance due to additional kinetic inductive effect which is insignificant at lower frequency .The slow wave propagation along conducting CNTs and the higher conductivity in comparison to metallic conductors like copper suggests them to be a preferred option for high frequency applications where the dimensions should be comparable to the propagation wavelength [18].

The bottleneck to the application of CNT as a TL section is the relative high characteristic impedance which may be reduced by introducing CNT bundles as a set of parallel single wall CNT. It has been agreed that CNTs are capable of carrying signals of Tetra Hertz frequencies [19-21].

The characteristic impedance of typical RLC network shown in Fig. 7 is expressed as:

$$Z = \sqrt{\frac{L}{C} - \frac{jR}{\omega C}} \quad (19)$$

The physical parameter based model for characteristic impedance may be derived by solving the above mentioned equation. The characteristic model for interconnect lengths greater than mean free path (l > λ), as scattering of electrons occurs beyond MFP may utilize the relation

$$|Z_0| = \sqrt{\frac{4\times10^3 l}{P_m n_{CNT} m}} \sqrt{1 + \frac{65\times10^4}{\omega^2}\left(\frac{1000}{1} + \frac{1}{d}\right)^2} \text{ where,}$$

$$m = \frac{C_E C_Q}{C_E + C_Q} \quad (20)$$

V. Characteristic Impedance Verification using SPICE

This work propose to utilize the above mentioned equation (20) to estimate the characteristic impedance of SWCNT bundle. The characteristic impedance for length greater than MFP is obtained w.r.t. variation in length and diameter of SWCNT bundle. The equations are validated against real life scenario of RLC circuit simulation using SPICE.

For current SPICE simulation, symmetrical circuit with image impedances at input and output are considered, known as characteristic impedance Z_0. The Z_0 of CNT interconnects is estimated with the proposed electrical equivalent model of unsymmetrical L-section transformed into symmetrical T-section [6] as shown in Fig.8.

VI. Characteristic Impedance as a Function of Length and Diameter

It is also intended to evaluate the variation of characteristic impedance as a function of length and diameter at constant frequency of 10 GHz which is represented as 3D plot in fig. 9 consolidating variation of characteristic impedance as a function of SWCNT bundle length and diameter. In this analysis CNTs of diameter 1nm, 1.5nm, 2nm, 2,5nm and varying length of 10µm, 15µm and 20µ are considered

VII. Transient Response of SWCNT Interconnects under Load Mismatch

The equivalent circuit in Fig. 7 is terminated at both input and output with Z0 derived as per equation (20) for different diameters and lengths of SWCNT bundle and the transient

response of the nanotube of the SWCNT bundle is presented in fig.10.

From fig.10 it is observed that if output impedance is matched to the impedance of the nanotube there is no ringing in the transient response output. The magnitude of critical mismatch variation in the impedance is given as in Table 1. The critical mismatching condition is estimated from the impedance at which the overshoot crosses 30% of the settled value and tabulated for varying lengths and diameters of interconnects. It is observed that the critical mismatching impedance of SWCNT is same for any length of interconnect but varies with diameter.

Table 1. Critical Mismatch Impedance for different length and diameters of Bundle SWCNT interconnects.

Bundle SWNT Interconnects	Diameter (nm)	Length of Interconnect (μm)		
		10	15	20
	1.0	4.35e+5 Ω	4.35e+5 Ω	4.37e+5 Ω
	1.5	5.14e+5 Ω	5.14e+5 Ω	5.14e+5 Ω
	2.0	5.70e+5 Ω	5.70e+5 Ω	5.70e+5 Ω
	2.5	6.20e+5 Ω	6.20e+5 Ω	6.20e+5 Ω

VIII. AC ANALYSIS OF SWCNT INTERCONNECTS UNDER LOAD MISMATCHES

The ac analysis of the circuit is conducted with input impedance matched with the impedance of the nanotube as transmission line and the output impedance varied to obtain 3 dB frequency (Hz) at critical mismatch which is presented in fig. 11.The result for the same is presented in fig. 11 and 3 dB frequency (Hz) at critical mismatch is presented in table 2.

Table 2. 3 dB frequencies of SWCNT bundle at Critical Mismatch Impedance for different length and diameters of Bundle SWCNT.

Bundle SWNT Interconnects	Diameter (nm)	Length of Interconnect (μm) Frequency (KHz)		
		10	15	20
	1.0	57.107	66.572	43.911
	1.5	86.122	94.552	64.427
	2.0	69.081	73.482	97.238
	2.5	100	57.417	48.165

CONCLUSION

The characteristic impedance of SWCNT bundle interconnects geometries are proposed as a function of physical parameters such as length, diameter and frequency while authenticating against SPICE simulated results. The results are presented through 3D graphs and Tables 1 & 2.Characteristic impedance variation is depicted as a function of diameter and length of interconnects at constant frequency with current model. The sole purpose of the same is to assist designers to realize compatible loading impedance for SWCNT bundle interconnects to reduce signal reflections and attenuations at minimum level. It is also aimed to estimate the range of frequencies that may be transmitted through these interconnects at different lengths and diameters under critical mismatch conditions.

ACKNOWLEDGMENT

This research paper has been solely made possible by the unconditional support of my family and few intellectuals who have really bestowed me with their presence in my life like Dr. R.P. Agarwal, Dr. B.K. Kaushik, Mr. Dinesh Chandra and Mr. Manoj Kumar Majumder. Their overwhelming support has always helped me to progress technically.

REFERENCES

[1] Francesco Ferranti,Giulio Antonini,Tom Dhaene,Luc Knockaert,and Antonio Orlandi, "Compact and Accurate Models of Large Single-Wall Carbon-Nanotube Interconnects", IEEE Transactions on Electromagnetic Compatibility, vol. 53, no. 4, November 2011.

[2] F. Kreupl, A. P. Graham, M. Liebau, G. S. Duesberg, R. Siedel, and E. Unger, "Carbon nanotubes in interconnect applications," Microelectron.Eng., vol. 64, pp. 399–408, 2002.

[3] F. Kreupl, P. Graham, M. Liebau, G. S. Duesberg, R. Seidel, and E. Unger, "Carbon nanotubes for interconnect applications," in Proc. Int. ElectronDevices Meeting Tech. Dig., 2004, pp. 683–686.

[4] N. Srivastava and K. Banerjee, "Performance analysis of carbon nanotube interconnects for VLSI applications," in Proc. IEEE/ACMInt. Conf.Comput.-Aided Des. 2005, pp. 383–390.

[5] K. N. Srivastava, H. Li, F. Kreupl, and K. Banerjee, "On the applicability of single-walled carbon nanotubes as VLSI interconnects," IEEE Trans.Nanotechnol., vol. 8, no. 4, pp. 542–559, Jul. 2009.

[6] Debaprasad Das and Hafizur Rahaman, Carbon Nanotube and Graphene Nanoribbon Interconnects. CRC Press Taylor & Francis Group, December 16, 2014 ISBN 9781482239485 - CAT# K23273.

[7] Jiang-Peng Cui, Wen-Sheng Zhao, Wen-Yan Yin and Jun Hu, "Signal Transmission Analysis of Multilayer Graphene Nano-Ribbon (MLGNR) Interconnects," IEEE Transactions on Electromagnetic Compatibility, vol. 54, no. 1, February 2012.

[8] Libao An, Xiaoxia Yang and Chunrui Chang, "On Contact Resistance of Carbon Nanotubes", International Journal of Theoretical and Applied Nanotechnology Volume 1, Issue 2, Year 2013 Journal ISSN: 1929-1248.

[9] N., Chiodarelli Y. Li, D.J. Cott, S. Mertens, N. Peys, M. Heyns, S.D. Gendt, G. Groeseneken, P.M. Vereecken, "Characterization of carbon nanotube via interconnects" 2011, Microelectron Engingeering, 88, 837-843.

[10] P. L. McEuen, M. Bockrath, D. H. Cobden, Y. G. Yoon,and S. G. Louie, Phys. Rev. Lett. 83, 5098 (1999).

[11] T. Ando and T. Nakanshini, J. Phys. Soc. Jpn. 67, 1704 (1998).

[12] P. L. McEuen, M. Bockrath, D. H. Cobden, Y. G. Yoon,and S. G. Louie, Phys. Rev. Lett. 83, 5098 (1999).

[13] Meninder S. Purewal, Byung Hee Hong,Anirudhh Ravi,Bhupesh Chandra,James Hone, and Philip Kim, "Scaling of Resistance and Electron Mean Free Path of Single-Walled Carbon Nanotubes", Phys. Rev. Lett. 98, 186808 (2007).

[14] International Technology Roadmap for Semiconductor 2013 Edition, available online at www.itrs.net.

[15] Roderick Jackson and Samuel Grahama ,"Specific contact resistance at metal/carbon nanotube interfaces" Applied Physics Letters 94, 012109 ,2009.

[16] Tersoff "Contact resistance of carbon nanotubes" 1999, Applied Physics Letters, 74, 2122-2124.

[17] Rochefort, P. Avouris, F. Lesage, D.R. Salahub "Electrical and mechanical properties of distorted carbon nanotubes" 1999, Physical Review Letters B, 60, 13824-13830.

[18] M. Attiya, "Lower frequency limit of Carbon Nanotube Antenna," Progress In Electromagnetics Research, PIER 94, 419,433, 2009.

[19] Naeemi and J. D. Meindl, "Design and performance modeling for single-walled carbon nanotubes as semi-global and global nterconnects in giga-scale integrated systems," IEEE Trans. Electron Devices, 54 (1), 26-37. (2007).

[20] Kaustav Banerjee and Navin Srivastava, "Are carbon nanotubes the future of VLSI interconnections," IEEE/ACM Design Autom. Conf. (pp. 809- 814). IEEE/ACM (2006)

[21] Manoj Kumar Majumder, Nisarg D. Pandya, B. K. Kaushik, and S. K. Manhas, "Analysis of MWCNT and Bundled SWCNT Interconnects: Impact on Crosstalk and Area," IEEE Electron Device letters, 33 (8), 1180-82 (2012)

Mr. Shailendra Mishra has done M.Tech (VLSI Design) from UPTU Lucknow and presently pursuing Ph.D. in CNT interconnects. He has a teaching experience of fifteen years and areas of interest includes VLSI design, Electromagnetism, Antenna and SPICE simulations. He has few papers in international journals and conferences to his repute.

(Dr.)R.P. Agarwal is currently working as Academic Advisor, Shobhit University, Meerut, India. He was former Vice Chancellor of Shobhit University, Meerut. Prof. Agarwal has rich varied experience of teaching, research, development and administration. He has 41 years of teaching experience and has published more than 100 research papers in **r**eferred International and National Journals

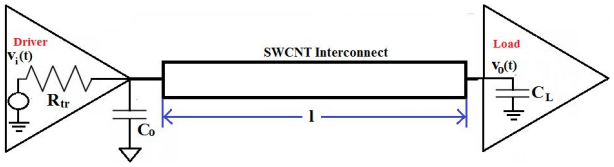

Fig. 1. Isolated SWCNT as Interconnect with driver and load positioning

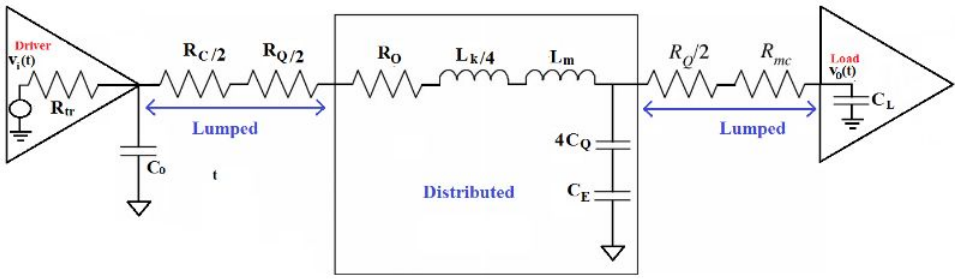

Fig. 2. TLM parameters along with driver and load parameters

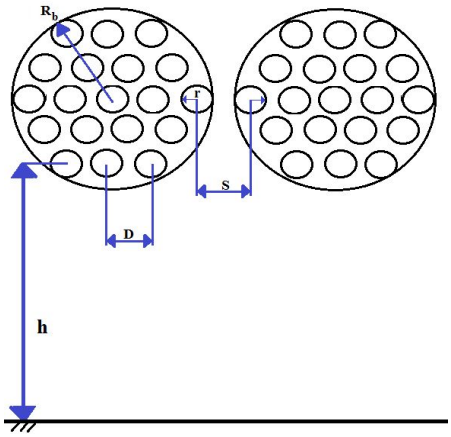

Fig. 3. Two SWCNT bundles above a ground plane with geometric configuration

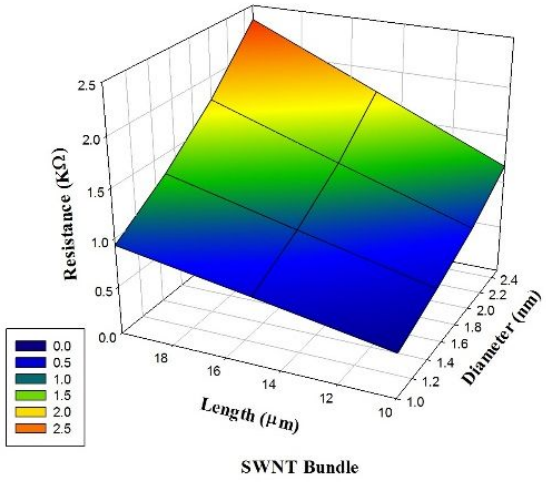

Fig. 4. A 3D plot of Impedance as a function of Length and Diameter for SWCNT Bundle interconnect for 22nm technological node.

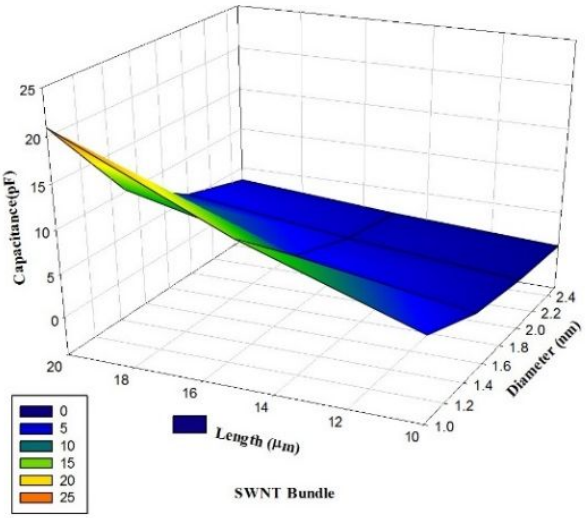

Fig. 5. A 3D plot of Capacitance as a function of Length and Diameter for SWCNT Bundle interconnect for 22nm technological node.

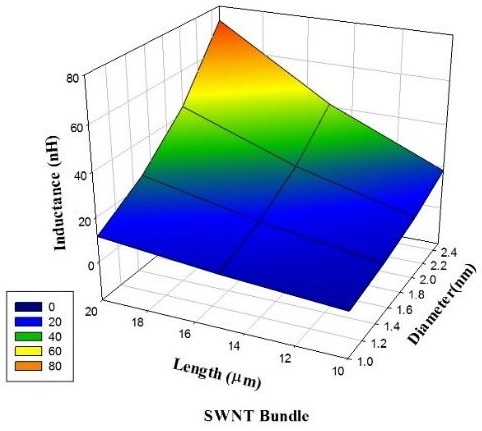

Fig. 6. A 3D plot of Inductance as a function of Length and Diameter for SWCNT Bundle interconnect for 22nm technological node.

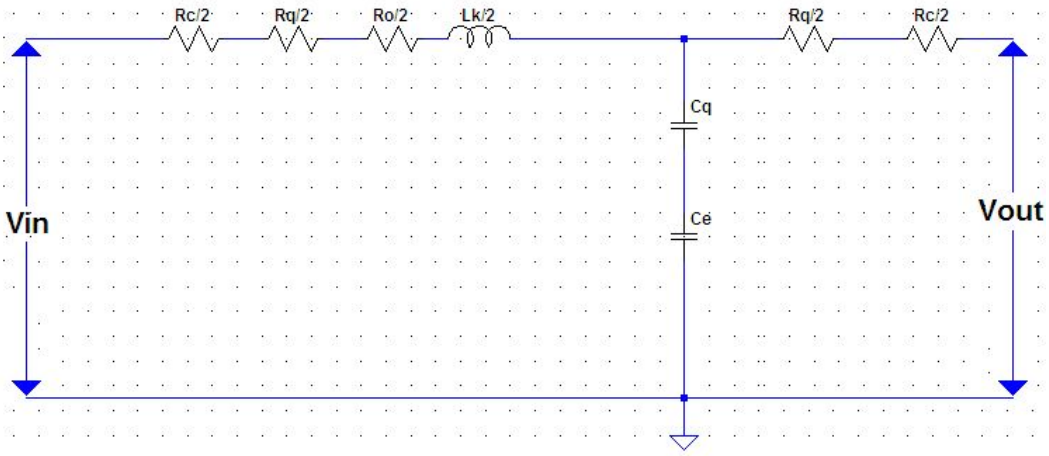

Fig.7. Equivalent circuit model of SWCNT interconnect.

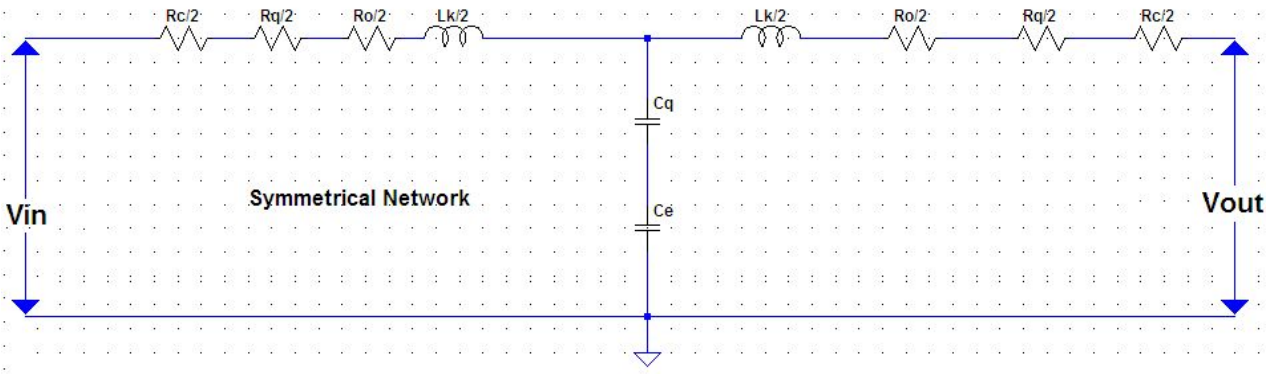

Fig.8.Equivalent Symmetrical T-section for Lumped SWCNT interconnect.

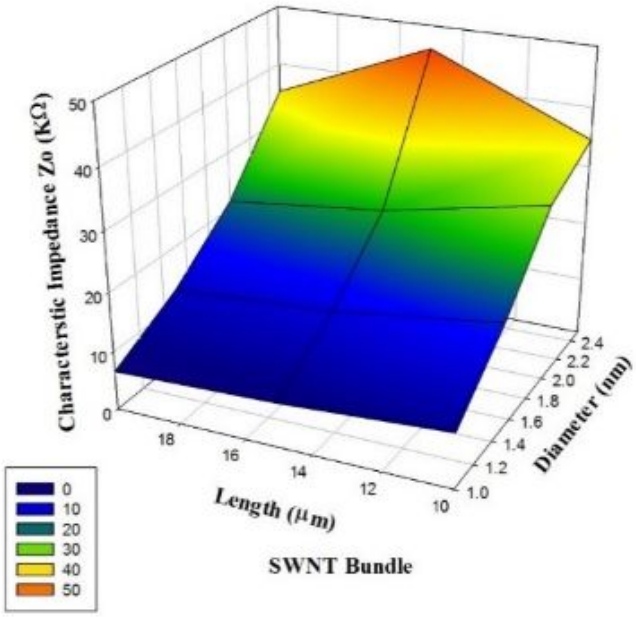

Fig. 9. A 3D plot of Characteristic Impedance as a function of Length and Diameter for SWCNT Bundle interconnect for 22nm technological node.

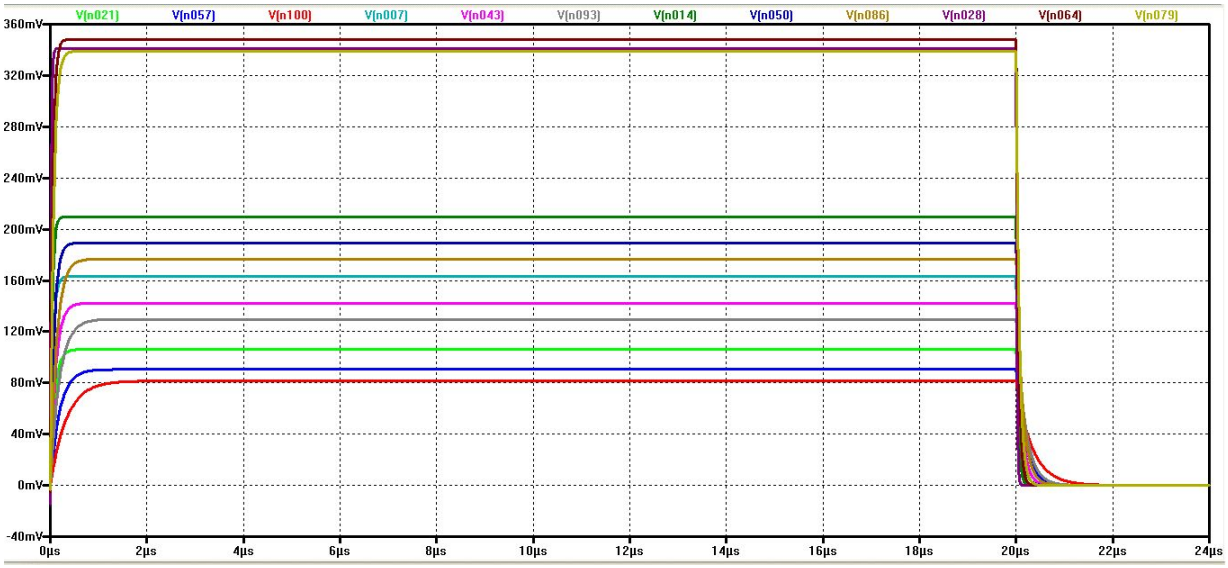

Fig. 10: Transient behavior of SWNT interconnects for matching conditions.

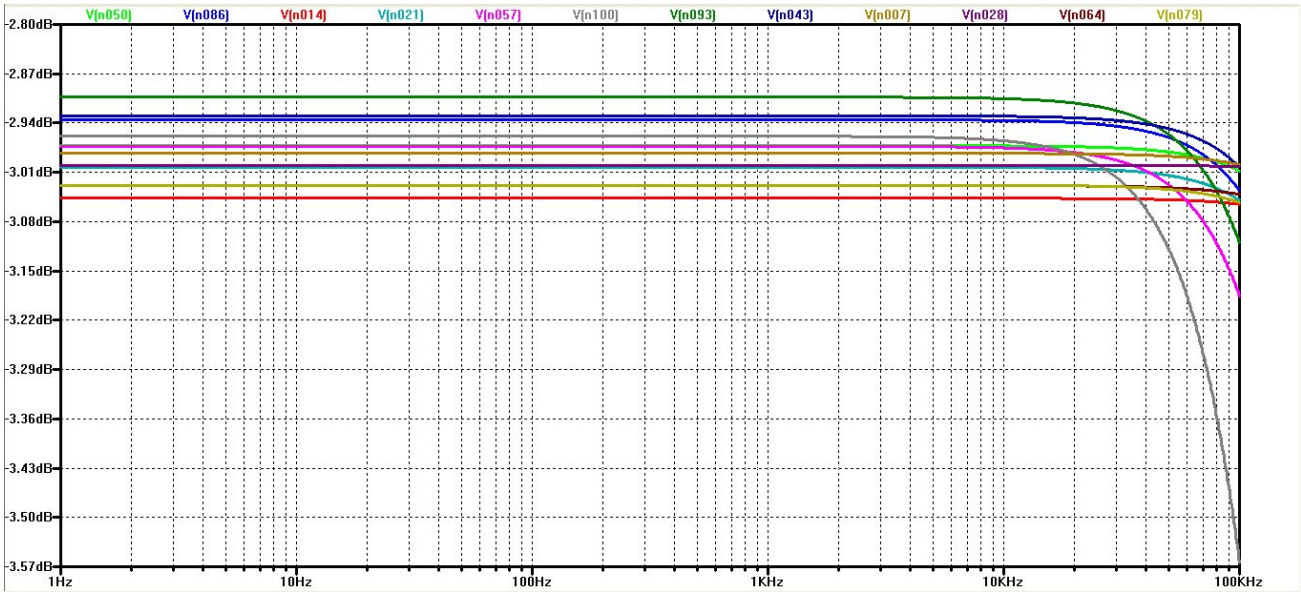

Fig. 11. Frequency Response of SWCNT for matching conditions.